A point-based scattering model for the incoherent component of the scattered field

Daniel C. Brown, Shawn F. Johnson, and Derek R. Olson

Citation: The Journal of the Acoustical Society of America **141**, EL210 (2017); doi: 10.1121/1.4976584
View online: https://doi.org/10.1121/1.4976584
View Table of Contents: https://asa.scitation.org/toc/jas/141/3
Published by the Acoustical Society of America

A point-based scattering model for the incoherent component of the scattered field

Daniel C. Brown,[a] **Shawn F. Johnson, and Derek R. Olson**
Applied Research Laboratory, The Pennsylvania State University, P.O. Box 30, State College, Pennsylvania 16804, USA
dan.brown@psu.edu, sfj102@psu.edu, dro131@psu.edu

Abstract: A numerical model for calculation of the incoherent component of the field scattered from random rough surfaces is described. This model is based on the point scattering approach, where the mean scatterer amplitudes are calculated from deterministic models. These amplitudes are then scaled by a complex circular Gaussian random variable to simulate scattering from a surface with minimal coherence length. The resulting simulated fields are shown to agree with theory for the mean field, mean square field, statistical distribution, and the spatial coherence length.

[DRB]
Date Received: September 30, 2016 **Date Accepted:** January 27, 2017

1. Introduction

Generation of spatially coherent time series for seafloor reverberation is useful for the investigation of several narrowband and broadband sonar system applications. Such a model may be used for generation of reverberation to investigate calibrated, or radiometrically accurate, synthetic aperture beamforming. Spatially coherent time series may also be used for the simulation of correlation velocity log sonar systems.

The coherent simulation of representative time series for the incoherent component of the field scattered from the seafloor may be approached using a number of simulation techniques. All properties of the scattered field can be achieved if a realization of a rough surface is generated, and the field is computed using a numerical solution of the appropriate integral equation governing the boundary value problem.[1] For example, this approach can be implemented using the boundary element method and is accurate given a fine enough resolution to achieve a specified tolerance. However, this accuracy is associated with significant memory and computational requirements. Approximations to the integral equation can be made, enabling considerable simplification. Pouliquen *et al.* developed such a technique using the Kirchhoff approximation.[2] Their approach is accurate so long as the rough surface is sampled finely enough (a discretized element should have a maximum linear dimension of $\lambda/8$), and the geometry and roughness statistics satisfy the assumptions used in the approximate model.

Additional simplification can be obtained if a representative scattered field is generated that has a number of statistical properties that are equivalent to those obtained from a scattered field due to realization of a rough interface. This approach has a different philosophy than the realization based approaches detailed above. Hunter developed this technique to simulate sonar imagery and he implemented it by discretizing the seafloor into patches that are large compared to the acoustic wavelength.[3] The scattered field from each patch for a given incident angle, scattered angle, and acoustic frequency is obtained by drawing a random variable from a distribution that has a specified two-point characteristic function. Hunter obtained this characteristic function through the use of the Kirchhoff approximation for the scattered field and a Gaussian roughness covariance function.

The point-based scattering model proposed in this work uses an approximation for the random draws on the scattered field, which allows greater flexibility in the selection of scattering models and roughness statistics without increasing the model complexity. Specifically the point-based scattering model assumes that the scattered field from neighboring points is independent. As with Hunter's technique, the proposed model aims to produce scattered fields with acceptable mean, variance, and covariance. The underlying assumption of independent scatterers leads to significant mathematical simplifications that allow efficient parallel implementation on multi-core computer systems.

[a]Author to whom correspondence should be addressed.

2. Point-based scattering model implementation

The point-based scattering model utilizes a finite number of discrete scattering centers that are distributed over a surface. These scattering centers are conceptually similar to a Rayleigh approximation in that the scatterers are much smaller than a wavelength and there is no multiple scattering. They are dissimilar to a Rayleigh approximation in that the scatterers have model-based aspect-dependent amplitudes and random phases. It is because of the combination of physical models and this complex, random scale factor that we describe the approach as "point-based" as opposed to being a point scattering model. For each scattering point, the transmitted field is scaled and then delayed by the round trip propagation time. The independent returns from all points are then coherently combined. Using the geometry in Fig. 1, the spectrum of the signal received from a collection of N scatterers is given by

$$P(\omega) = S_0(\omega) \sum_{n=1}^{N} b_T(\psi_T, \omega) b_R(\psi_R, \omega) a(\theta_i, \theta_s, \phi, \omega) \frac{e^{ik(R_T+R_R)}}{R_T R_R}, \tag{1}$$

where S_0 is the transmit spectrum, b_T is the transmit directivity function, b_R is the receive directivity function, k is the wavenumber, and a is the scatterer amplitude. A separate term for attenuation in the water column has been omitted; however, it could easily be added. The associated time series are generated through an inverse Fourier transform of this expression. Note that while each of the terms within the sum is calculated independently for each scatterer, the subscript n has been omitted for notational simplicity. The form of this equation assumes propagation in a uniform medium. The directivity functions b_T and b_R may be given either by equations for the far-field directivity for transducers or by direct measurements from actual hardware. The scatterer amplitude a consists of both deterministic and stochastic components. The root-mean-square of a is determined by the local scattering strength of the seafloor and the mean density of the scatterers. A stochastic term, ζ, is included to ensure the field scattered from any pair of points is incoherent. The scatterer amplitudes are given by

$$a(\theta_i, \theta_s, \phi, \omega) = \zeta \sqrt{\frac{\sigma(\theta_i, \theta_s, \phi, \omega)}{\rho_s}}, \tag{2}$$

where ρ_s is the scatterer density with units scatterers/m^2, σ is the dimensionless bistatic differential cross section per unit area per unit solid angle, and ζ is a complex, unitless, scale factor. The effect of bottom roughness is accounted for through this differential cross section, and it is calculated from a bottom roughness scattering model. In this work, the small-slope approximation has been implemented for the modeling results discussed in Sec. 3.[4] A simpler model for the bistatic cross-section could be substituted as well. Note that multiple scattering and shadowing may be significant at very low grazing angles, although these effects are not included in this model. The scale factor ζ is given by

$$\zeta = (X + iY)/\sqrt{2}, \tag{3}$$

where X and Y are independently distributed standard normal random variables. The inclusion of this term assumes that the field scattered from any pair of scatterers is

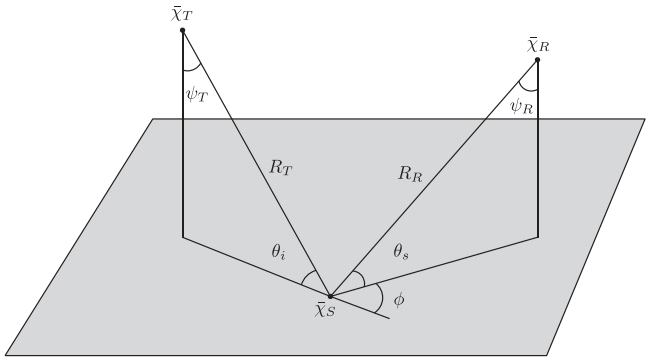

Fig. 1. The field projected by a transmitter at $\bar{\chi}_T$ is scattered from a point at $\bar{\chi}_S$ and is received at $\bar{\chi}_R$.

incoherent. Jackson and Richardson note this is a reasonable approximation if the true surface pressure correlation length is sufficiently small and the source and field points are sufficiently far from the scattering surface.[5] If the surface pressure correlation length is not sufficiently small, then the random variable ζ must have some spatial correlation.

3. Model-to-model comparisons

The mean field, mean square field, and spatial coherence length of the signals generated by the point-based model are compared to theoretical values provided by the narrowband sonar-equation model. The mean field and mean square field are compared to the sonar equation over a wide range of grazing angles for a sensor near the seafloor. The spatial coherence of the simulated fields is compared to the result predicted by the van Cittert-Zernike theorem for a sensor with a much greater standoff.

To evaluate the mean and mean square fields, 100 pings have been simulated for a monostatic sonar system operating 3 m above a medium sand seafloor. Because the output will be compared to a narrowband sonar equation, the beampattern and scattering strength are assumed to be frequency invariant in these simulations. The transmitter and receiver are both directed at normal incidence and each has a Gaussian beampattern given by $b(\psi) = \exp[-\psi^2/2\psi_0^2]$. The -6 dB width of the beam is set to 120° by setting $\psi_0 = 51°$. The transmitted waveform is a 200 μs sine wave at 10 kHz. The water is assumed to have a sound speed of 1500 m/s and a density of 1000 kg/m^3. The interface is populated over a 60 m $\times$ 60 m area with $\rho_s = 2500$ scatters/m^2. This creates a linear scatterer density of 7.5 scatterers per wavelength, which is near that used by Pouliquen. The sediment's geoacoustic and roughness parameters were selected to be representative of medium sand.[6] The sediment density is 1845 kg/m^3, the compressional wave speed is 1767 m/s, and the compressional wave attenuation is 0.89 dB/λ. The roughness is assumed to follow a power law spectrum, $W(k_r) = wk_r^{-\gamma}$, where k_r is the horizontal radial wavenumber, $w = 1.41 \times 10^{-4}$ m$^{4-\gamma}$ is the spectral strength, and $\gamma = 3.25$ is the spectral exponent.

A narrowband estimate of the expected level for the mean square field is given by the sonar equation for a given sensor and environment. This equation for a monostatic sonar is

$$\langle |P(t)|^2 \rangle = 2\pi\sigma(\psi)\frac{R_+^2 - R_-^2}{R^4}|b(\psi)|^2, \tag{4}$$

where

$$R_\pm = \sqrt{\frac{c}{2}\left(t \pm \frac{\tau}{2}\right) - z^2}, \tag{5}$$

is the inner and outer edges of the scattering annulus and τ is the length of the pulse.[5] In Fig. 2, the 100 ping ensemble of the mean square field is compared to the sonar equation. The agreement is good over nearly the full temporal range, and the only disagreement is near the onset of the signal at 4 ms. Near this time, the scattering strength, which is assumed to be invariant in Eq. (4), varies over the annulus of the seafloor within the pulse length.

The formally averaged value of the incoherent component of the scattered field is zero by definition. The expected mean level for a 100 ping ensemble is $10\log_{10}(1/100) = -20$ dB below the signal level without averaging. The envelope of the mean field, $|\langle P \rangle|^2$, is compared to the sonar equation less 20 dB in Fig. 2. Again the agreement is quite good over nearly the full range of the signal.

At any instant in time, the pressure should follow a normal distribution with zero mean and variance proportional to the sonar equation. To test this, the samples in the ensemble from 20 to 40 ms have been normalized by the sonar equation. This subset was selected because the validity of the sonar equation normalization improves with increasing range. Through normalization the sampled pressure is transformed to a standard normal distribution whose properties should be invariant with time. In Fig. 3(a), a quantile-quantile plot is shown and the samples are seen to fall along the diagonal indicating the normalized data are drawn from a standard normal.

An idealized configuration has been simulated to compare the spatial coherence of the scattered field to theory. The approximations made in this part of the analysis are non-physical in nature; however, they permit a comparison of the scattering model to an analytic expression for the spatial coherence that may be derived from the van Cittert-Zernike theorem.[7] A sonar is simulated 150 m above a uniform disk of

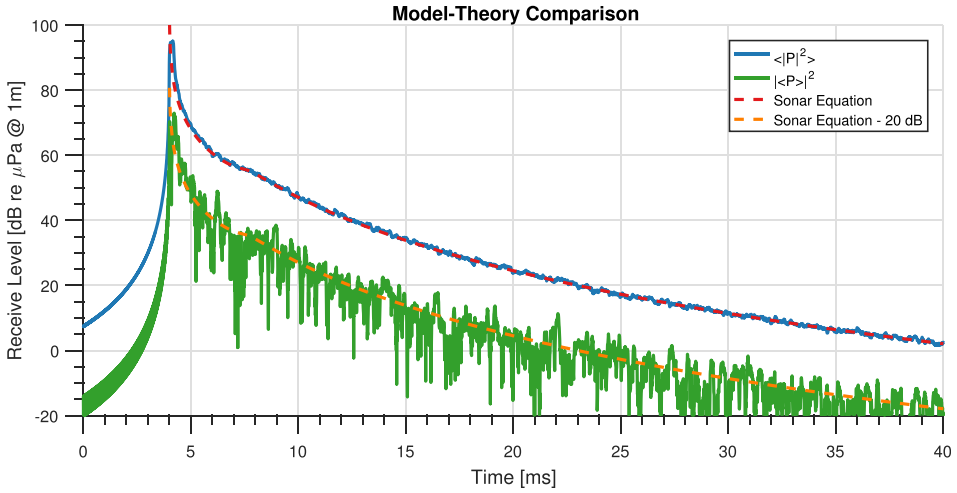

Fig. 2. (Color online) The envelope of the mean field, $|\langle P\rangle|^2$, and mean square field, $\langle|P|^2\rangle$, are shown for a 100 ping ensemble at normal incidence. They are each compared to the narrowband sonar equation [Eq. (4)].

scatterers that is 35 m in diameter. The scatterers are modeled as having a uniform, aspect-independent, scattering strength. The sonar consists of a single omnidirectional transmitter adjacent to a line array of omnidirectional receivers with an inter-element spacing of 9.1 cm. The transmitted waveform is a 1 ms sinusoid at 20 kHz. Losses due to spreading have been ignored. Given these assumptions, the field is scattered from a

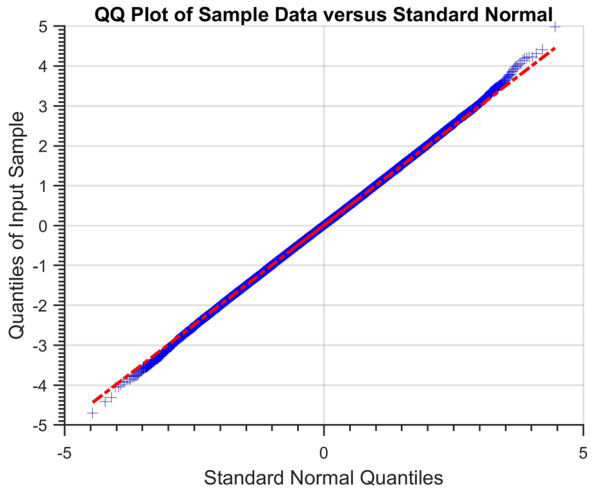

(a)

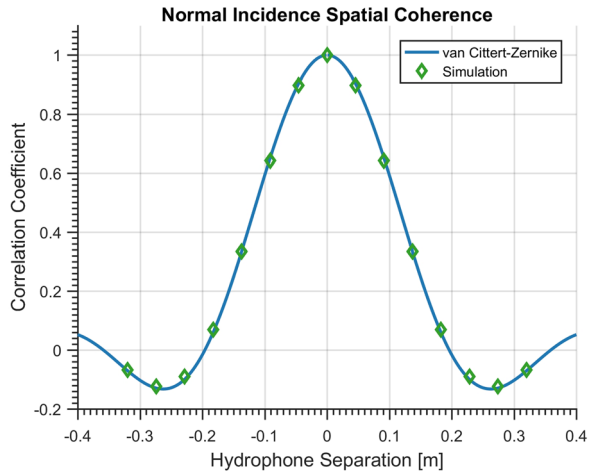

(b)

Fig. 3. (Color online) The normalized data are shown to follow a standard normal distribution in (a). The spatial coherence of scattered field is compared with the van Cittert-Zernike theorem for an idealized environment in (b).

uniform mean amplitude, incoherent disk ensonified by a far-field source. An analytic expression for the spatial coherence of the field scattered from such a disk is given by the van Cittert-Zernike theorem.[7] Expressing this spatial coherence as a spatial correlation coefficient gives

$$\mu_{12}(\Delta l) = \frac{J_1\left(\frac{2\pi a}{\lambda d}\Delta l\right)}{\frac{\pi a}{\lambda d}\Delta l}, \tag{6}$$

where $J_1()$ is the Bessel function of the first kind of order 1, a is the radius of the scattering disk, d is the range to the seafloor, λ is the wavelength, and Δl is the spatial separation for any hydrophone pair.

The point-based scattering model has been used to form a 100 ping ensemble for this sensor and environment. The correlation coefficient is calculated between all pairs of channels in the receive array for each ping. The correlation coefficients calculated from a single ping will have redundant spatial offsets.[8] These redundant offsets are averaged, and then the average correlation coefficient is calculated across the simulated ping ensemble. The simulation is compared to Eq. (6) in Fig. 3(b). The discrete spatial sampling of the simulated receive array produces a discrete spatial sampling of the correlation coefficient. The agreement is good between the correlation coefficient predicted by the van Cittert-Zernike theorem and the point-based scattering model. This result is similar to that found by Jackson and Morovan for the simulation of coherence of scattering from the air-water interface using a Point Scattering model.[9]

4. Conclusion and future work

A time series model for the incoherent component of the field scattered from a random rough surface has been developed. This is a point-based scattering model, where the individual scattering amplitudes are set by deterministic physical models as well as a stochastic scale factor. The model has a mathematically simple form which allows easy implementation. The results of this model have been compared to the sonar equation, and both the mean field and mean square field show good agreement. The spatial coherence of the scattered field was also shown to agree with the van Cittert-Zernike theorem for an idealized environment. Additionally, the data are shown to follow the proper statistical distribution.

There are several areas of future work to be explored. The model presented here provides a simulation of only the incoherent component of the scattered field. A separate model for the coherent component is required to simulate the complete field scattered from a rough interface. Additionally, the simulations examined here used an average scatterer density of 7.5 scatterers per wavelength. This number was chosen to roughly match the density of facets used in the model developed by Pouliquen *et al.*[2] At this density of scatterers, simulation of the field scattered from large areas at high frequencies can result in extremely large numbers of scatterers. Work should be conducted to determine what minimum scatterer density is needed to produce fields with the appropriate properties. Finally, work should be conducted to better understand and model the role of seafloor roughness and texture, in combination with the required scatterer density, on the stochastic scatterer scale factors [i.e., Eq. (3) in this work].

Acknowledgments

This research is supported in part by the U.S. Office of Naval Research (ONR). This research was supported in part by the U.S. Department of Defense, through the Strategic Environmental Research and Development Program (SERDP). This material is based upon work supported by the Humphreys Engineer Center Support Activity under Contract No. W912HQ-16-C-0006.

References and links

[1]O. Steinbach, *Numerical Approximation Methods for Elliptic Boundary Value Problems* (Springer, New York, 2008).
[2]E. Pouliquen, O. Bergem, and N. G. Pace, "Time-evolution modeling of seafloor scatter. I. Concept," J. Acoust. Soc. Am. **105**, 3136–3141 (1999).
[3]A. J. Hunter, "Underwater acoustic modeling for synthetic aperture sonar," Ph.D. thesis, University of Canterbury, Christchurch, New Zealand (2006).
[4]R. F. Gragg, D. Wurmser, and R. C. Gauss, "Small-slope scattering from rough elastic ocean floors: General theory and computational algorithm," J. Acoust. Soc. Am. **110**, 2878–2901 (2001).
[5]D. R. Jackson and M. D. Richardson, *High Frequency Seafloor Acoustics* (Springer, New York, 2007).
[6]APL-UW, "APL-UW high-frequency ocean environmental acoustic models handbook," Technical Report TR 9407, Applied Physics Laboratory—University of Washington (1994).

[7]J. W. Goodman, *Statistical Optics* (John Wiley and Sons, New York, 1985).
[8]P. J. Boltryk, M. Hill, A. C. Keary, and P. R. White, "Surface fitting for improving the resolution of peak estimation on a sparsely sampled two-dimensional surface with high levels of variance, for an acoustic velocity log," Meas. Sci. Technol. **15**, 581 (2004).
[9]D. R. Jackson and K. Y. Moravan, "Horizontal spatial coherence of ocean reverberation," J. Acoust. Soc. Am. **75**, 428–436 (1984).